THE UNIVERSITY OF MICHIGAN

INDUSTRY PROGRAM OF THE COLLEGE OF ENGINEERING

NATURAL CIRCULATION EXPERIMENTS IN AN OSCILLATING FORCE FIELD

John B. Woodward III
Herman Merte, Jr.

November, 1965

IP-722

TABLE OF CONTENTS

LIST OF FIGURES

INTRODUCTION

This paper presents results of an experimental study of some aspects of two-phase natural circulation fluid flow and heat transfer in a system which is mounted on an oscillating carriage. The purpose is to simulate the behavior of a steam generator operating aboard ship, and thus subjected to motions of the ship hull.

The driving head in natural circulation is proportional to the product of the body force due to gravity and a density difference. If the system is in motion, an additional body force due to the vertical component of the acceleration is superimposed on the gravity force. The hull of a ship undergoes motions caused by wave action; the vertical component is designated heave, and is approximately periodic. Hence, the natural circulation steam generating circuits in a marine boiler are subjected to a periodic driving head. When the driving head is periodic, it might be anticipated that the instantaneous flow rate would surge periodically in response. The possibility of periodic surge in itself may scarcely warrant experimental verification, but possible consequences of the surges are more speculative. The principal ones are:

1) Changes in the net flow rate, or in the net vapor generation rate.

2) Fluctuations in the temperature of the tube wall.

3) Lowering of the burnout heat flux.

4) Fluctuations in the vapor void fraction.

None of these factors appear to be of present concern to the marine boiler industry. As far as the authors are aware, contemporary

boiler designers take no account of ship motion influence on circulation and heat transfer. On the other hand, possible motion effects have been a major concern to designers of several proposed direct-boiling marine nuclear steam generators (1)*. The reason for the contrast is that heat fluxes are inherently higher in nuclear reactor cores than in combustion boilers, and that void fraction changes may actually be hazardous in the reactor because of the void fraction effect on reactivity. Consequently, the reports of previous work in this field come exclusively from nuclear power development programs.

Experimental work similar to that reported here has been done in the United States, Norway, and Japan. American work has included operation of a circulating loop mounted on a swinging framework to simulate rolling motion (1,2). The Norwegians have operated a vertically oscillating loop (3). Flow surge data (1,2,3) and void fraction data (3) is reported, but no information is available on the influence of oscillation on burnout heat flux or tube wall temperature. Mass flow rate, burnout heat flux, and void fraction data are reported in Japan for vertically oscillated test loops containing several types of simulated reactor fuel elements (4). In this work, the resonant effect in burnout heat flux, such as is reported here, was not observed.

Water was used as the working fluid in all these programs. In the work reported here, the fluid is freon-11. Use of freon-11 allows simulation of high pressure water behavior by low pressure operation. The principal parameter determining natural circulation behavior is the liquid-vapor density ratio, which, for example, is the same for freon-11 at

* Numbers in parenthesis refer to similarly numbered references in bibliography at end of paper."

100 psia (P_r = 0.157) as for water at 680 psia (P_r = 0.212). Enthalpy of vaporization is lower by an order of magnitude in freon-11, hence burnout heat fluxes are lower by about the same ratio than in water. It is shown later that a burnout heat flux correlation which includes density ratio and enthalpy of vaporization works well with either fluid.

The natural circulation circuit tested here is not intended to model any particular type of steam generator. However, the circular-tube geometry more closely resembles a combustion boiler circuit than a nuclear reactor core. The L/D ratios of downcomer and riser are similar to those of a marine boiler. The range of peak accelerations used is believed to cover those likely to be encountered aboard ship. The frequencies of the imposed motion were selected to include the natural frequency of the flow system, and do not necessarily represent a realistic range for a ship.

The independent parameters varied in this work are system pressure, heat input rate, frequency and stroke length of the imposed motion, and downcomer flow resistance. Pressures used are 50, 75 and 100 psia. Heat input rates cover a range from 6000 to 50,000 BTU/hr-ft^2. Motion frequencies cover a range from 29 to 94 cycles/min, and stroke lengths are 4, 8, 12 and 16 inches. Maximum accelerations of the carriage are $\pm$ 1.0g ($0 \leq a_{MAX} \leq 2$) . Downcomer flow resistance is adjusted by means of a rotating plug type valve. Plug rotations of 0°, 35°, and 50° (75° is fully closed) are used, but unless otherwise stated, data presented refers to wide open condition, 0° plug rotation. Subcooling of liquid at the heated section entrance is not varied, but is maintained at $15^{+}_{-} 3$ degrees for all test runs.

Measurements are made of mass flow rate, heat input rate, system pressure, acceleration, fluid temperature at entrance and exit of heating section, and of outer surface temperatures along the heating tube.

DESCRIPTION

The principal components of the natural circulation loop are shown in Fig. 1. The loop is mounted on a carriage which is oscillated within vertical guides by a connecting rod, crank arm, flywheel, speed reducer, and motor. The speed can be varied continuously from 0 to 130 RPM. The loop is constructed of copper, pyrex, and stainless steel tubing, all approximately 7/16 inch I.D. Cooling water is circulated through a coil in the vapor separation drum to condense the vapor, with flow adjusted by a manual valve to balance heat input and output of the system, and thus maintain the desired system pressure.

Temperatures are measured by calibrated iron-constantan thermo-couples, 16 being welded at two-inch intervals to the outer surface of the heated test section, and one each inserted into the fluid at inlet and outlet of this section. Thermocouple EMF is recorded on an oscil-lograph recorder with adequate frequency response. Heating is accomplished by passing direct current through the walls of part of the riser, with current and voltage being measured to determine heat flux. Instantaneous acceleration of the carriage is recorded with a $\pm$ 2g strain gage accelero-meter. System pressure at the lower header is recorded with a 0-200 psig strain gage transducer. A 0-200 psig Heise gage is also installed for calibration of the transducer. Mass flow rate is recorded by means of a venturi, near the bottom of the downcomer, with a strain gage ΔP trans-ducer. Both pressure transducers are carefully positioned so that carriage acceleration does not induce false signals.
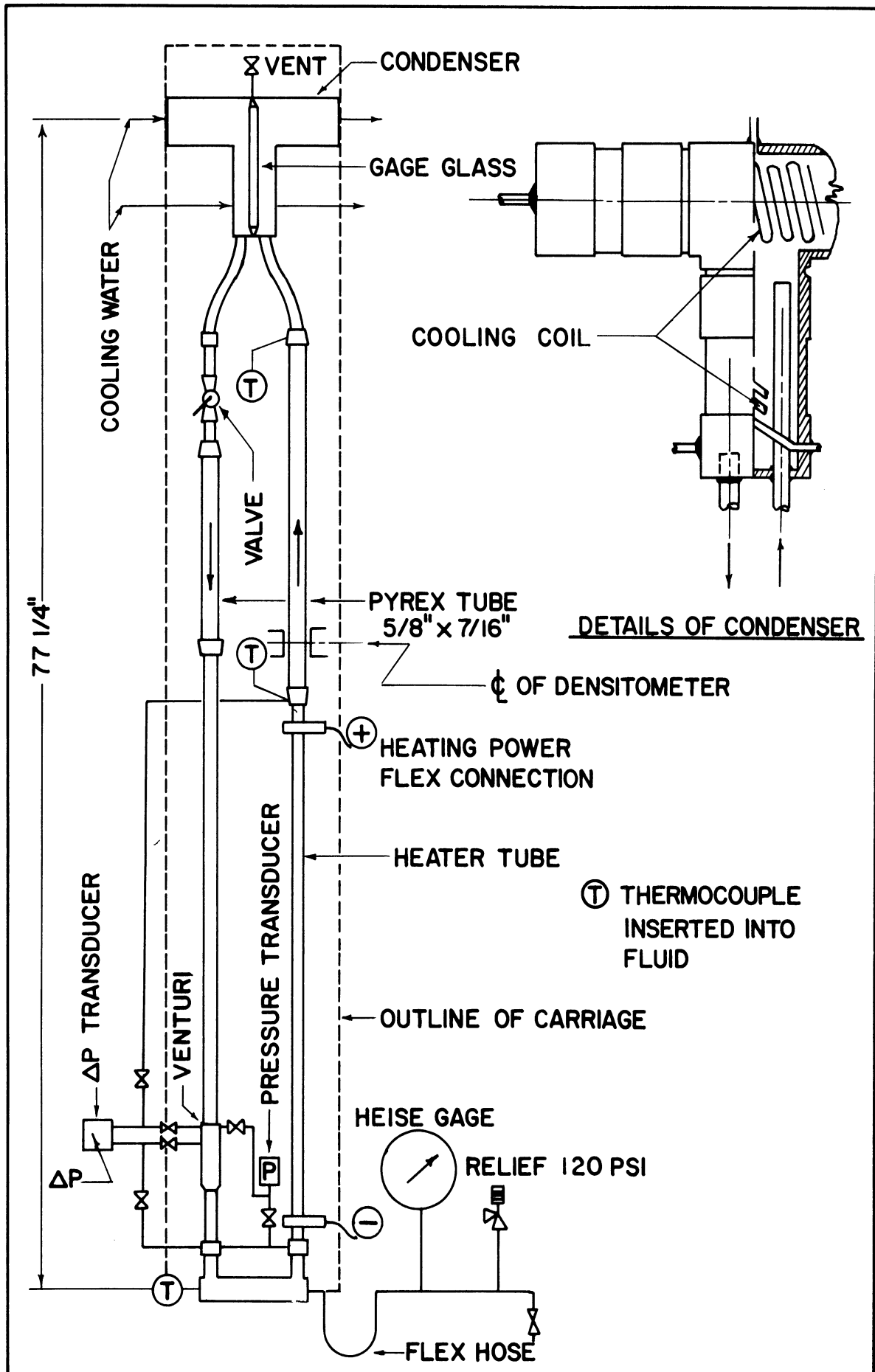
Figure 1. Arrangement of Natural Circulation System.

Void fraction in the riser ten inches above the heated section is measured by a gamma ray attenuation densitometer which moves with the carriage. The basic elements of this instrument are a thullium-170 gamma-ray source, collimator, scintillation crystal - photomultiplier assembly, preamplifier, and decade scaler. This instrumentation is similar to that frequently used to measure void fraction in water systems (5,6,7). An additional element introduced for motion measurements is a timed gate in the signal path between photomultiplier and scaler. This device closes the signal circuit at a definite point in each cycle of the carriage, and keeps it closed for a definite fraction of the cycle. It is tripped by a trigger pulse from a microswitch actuated by one of eight equally spaced cams on the flywheel. The microswitch can be shifted to engage any one of the eight; hence, an interval of signal passages can be set at eight different points in the motion cycle. In taking data, the system is operated until sufficient counts have reached the scaler to reduce statistical uncertainty to the desired level.

Further details of the experimental apparatus appear in Ref. 8.

DATA REDUCTION

Steady mass flow rate is calculated from the flowmeter ΔP signal. When flow is unsteady, a correction is made for the component of ΔP caused by acceleration of fluid between the taps. Uncertainty in mass flow measurement is $\pm$ 14% at the lowest average flow rates used (300 lbm/hr) and $\pm$ 4% at the highest average flow rate (700 lbm/hr).

Steady heat flux is calculated from the measurements of current and voltage, with the uncertainty in the result estimated to be $\pm$ 1% . When the flow of fluid within the tube oscillates, wall temperatures oscillate also. Surface heat flux therefore must oscillate also, since heat generation rate remains steady while the tube wall is absorbing and releasing heat due to its thermal capacity. The instantaneous heat flux is calculated from the difference between heat generated and heat stored by the relation

$$q'' = q_N'' - \rho_m C_m \delta \frac{dT_m}{dt} \tag{1}$$

The derivative $\frac{dT_m}{dt}$ is taken from the slope of the outer surface thermocouple traces, since it had been analytically determined that for this application the rate of temperature change is very nearly the same throughout the thickness of the wall.

Uncertainty in temperature is estimated to be $\pm$ 1°F for the fluid temperature measurements when readout is taken on the recorder. The thermocouples measuring tube wall temperature are subject to error caused by voltage in the wall between the points of attachment of the iron and constantan wires. The error is found by calibration, with the uncertainty

in outer wall temperature subsequently estimated to be ± 2°F.

Temperatures at the inner surface of the heating tube wall are calculated from the temperatures measured at the outer surface. In the steady state this is done by solution of the steady-state diffusion equation with boundary conditions of known temperature and zero gradient at the outer surface. When the outer temperature is unsteady, i.e. displaying periodic fluctuations in response to oscillating flow, the calculation proceeds as follows:

1) A harmonic analysis is applied to resolve the outer temperature trace into sinusoidal components.

2) The attenuation and phase shift for each component in passing through the wall is calculated by solving the heat diffusion equation with sinusoidal input. The amplitude and phase position of each component at the inner surface is thus known.

3) These inner surface components are summed to produce the temperature trace.

Carriage acceleration is calculated from its frequency and position, with accelerometer measurements being used to observe frequency and smoothness of the motion.

Burnout is detected by an abrupt change in one or more wall surface temperature traces from steady or unsteady-periodic behavior to a continuous rapid rise. Such an event is shown in Fig. 2. Calculations indicate that a negligibly small time lag exists between changes in inner and outer surface temperatures, and this rise is considered to occur simultaneously at inner and outer surfaces. In accord with the method of
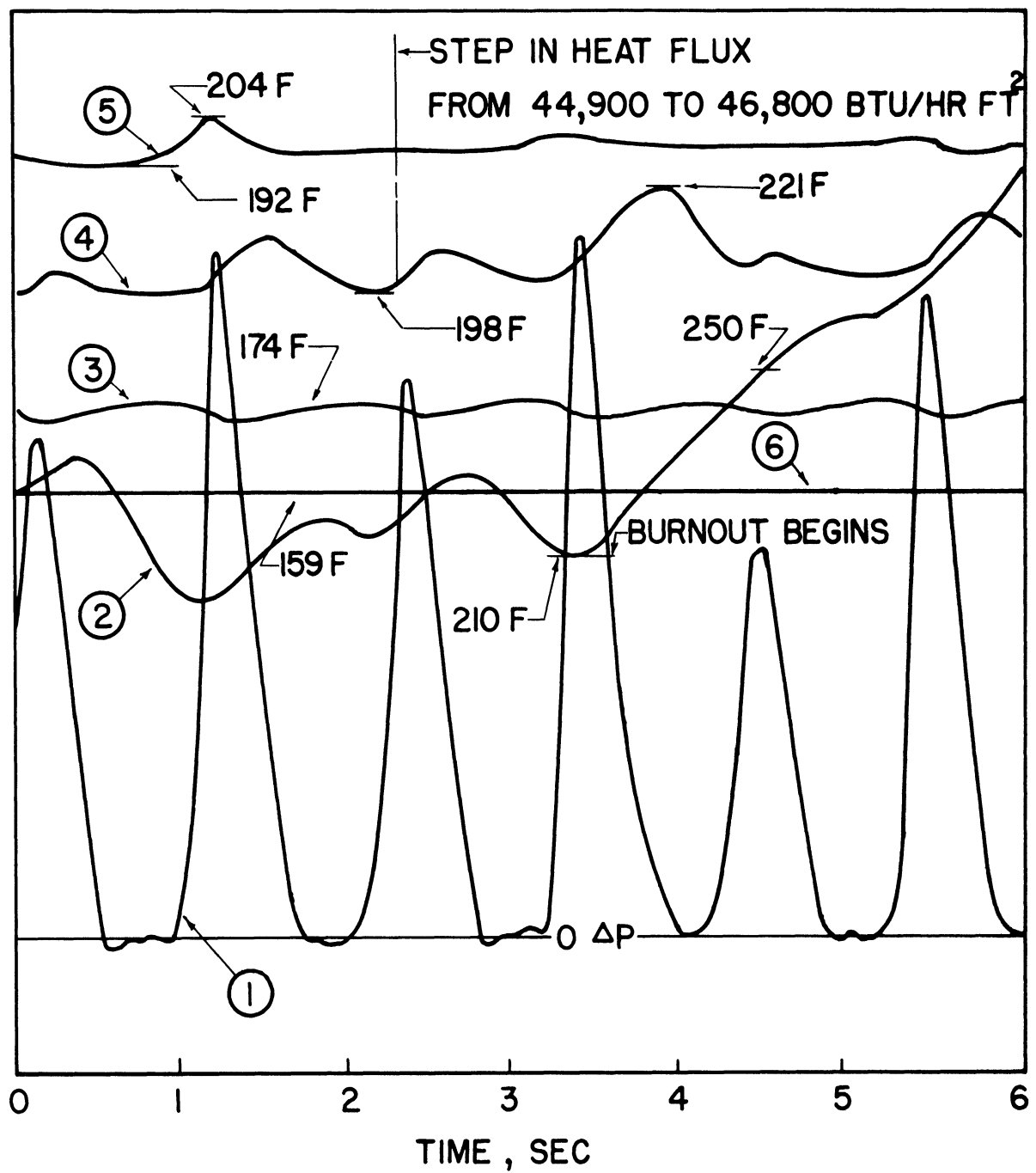
Figure 2. Recorder Chart of Natural Oscillation Flow and Temperature.

detection, the term "burnout heat flux" used here is the value of the time average heat flux at which the outer surface temperature begins a continuous rapid rise.

Void fraction is found from the densitometer reading by:

$$\alpha = \frac{\log C/C_f}{\log C_g/C_f} \tag{2}$$

Eq. (2) is widely used in void fraction measurement (e.g. Ref. 5-7).

Void fraction data was taken by a "one shot" method, using a single reading of a 1/16 inch wide beam along the tube diameter. This represents the average void fraction only if the distribution of voids across the tube is uniform. Correction factors are applied to the one shot data, determined by calibration for each condition by traversing the densitometer beam across the tube, translating the results into void fraction as a function of radius, and then integrating to find the average. The calculation of void fraction as a function of radius uses the method developed by Hammitt, et al. (9).

Uncertainty in void fraction is estimated to be $\pm$ 5% at α = 1.00 , and 7% at α = 0.60 , the lowest encountered.

Slip ratio in steady flow is calculated (e.g. Ref. 6,7) by:

$$S = \frac{x}{1-x} \frac{1-\alpha}{\alpha} \frac{\rho_f}{\rho_g} \tag{3}$$

STATIC FLOW RESULTS

The term _static_ is used to denote conditions existing with the carriage stationary. All data taken with the system oscillating was first taken in the static condition for purposes of comparison.

Mass Flow Rate

Static mass flow rate data for system pressures of 50, 75, and 100 psia with wide-open flow valve is presented in Fig. 3. The principal features are an initial increase of the flow rate as the heat input is raised, a maximum that is approximately the same for all pressures, and a subsequent decrease as heat input is raised further, but with a steeper decrease for the lower pressures. The flow rate for each pressure reaches a point beyond which it decreases no further as heat flux is raised. The flow does, however, become oscillatory near this point, and the amplitude and frequency of the flow rate oscillations increase with increasing heat flux.

Calculated mass flow rates are also plotted in Fig. 3, and agreement with the experimental results is good except where the flow becomes oscillatory. The method of calculation is based on the principle that pressure differences around the loop must total zero. Pressure drops caused by friction and acceleration (in the heated section) are equated to the driving head due to density differences between riser and downcomer. Details of the calculations are found in Ref. 8.

Flow oscillation at high heat flux is typical of natural circulation loops (10,11). It is of particular significance in this work because of the possibility of resonance between this oscillation and the carriage
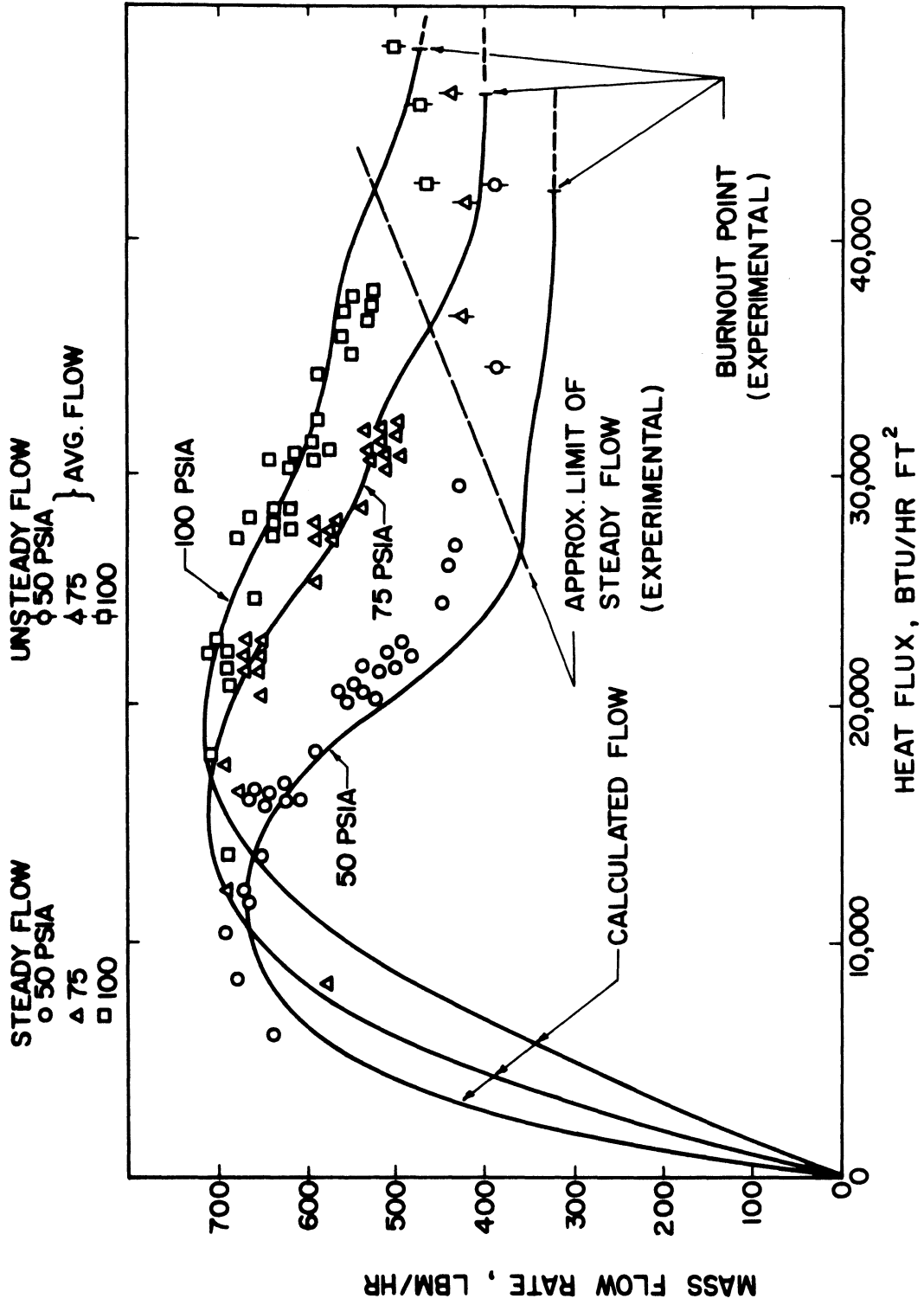
Figure 3. Static Mass Flow Rate.

motion. It is later seen that this resonance does occur, and that its effects are evident even at levels of heat flux below that which causes natural oscillation. In application it is generally desirable to avoid resonance, and a means of calculating the natural frequency and heat flux at which oscillation begins, is thus necessary. An extensive literature on methods for doing so exists (e.g.(12-14)). An additional method of analysis has been developed as part of this program, and will be the subject of a future paper.

The effect of flow valve closure, and hence downcomer resistance, on static mass flow rate is small up to about 40° (F_c = 1.0) plug rotation. At 50° (F_c = 0.5) rotation, the maximum flow is about 40% of the 0° rotation (F_c = 8.5) maximum flow. The valve is fully closed at 75° rotation. The effect of its closure is to increase slightly the heat flux at which the natural flow oscillation begins, and to decrease the amplitude of the oscillation. At approximately 50° closure, the amplitude is reduced to zero and mass flow rate is steady up to the burnout point.

Burnout Heat Flux

Burnout heat flux as a function of system pressure and of flow valve position are presented in Table I. Flow rate is oscillatory when burnout occurs in all cases except for the 50° valve position, and for 35° valve position at 100 psia. Time average heat flux values are given in all cases. The values tabulated are mean values of many data points. Scatter of this data is small, 90% of the data points being within ± 1% of the mean.

TABLE 1

BURNOUT HEAT FLUX DATA

VALVE POSITION	0°			20°			35°			50°		
SYSTEM PRESSURE	50	75	100	50	75	100	50	75	100	50	75	100
MASS FLOW RATE	4.60	4.65	4.50	4.20	4.30	4.20	3.65	3.65	3.90*	2.50*	2.80*	3.00*
PREDICTED q''_{BOO}	71,700	69,500	64,200	68,600	66,300	61,700	62,700	59,800	59,000	48,000	49,900	49,500
ACTUAL AVG q''_{BOO}	42,700	46,400	48,100	42,300	46,000	48,800	44,200	51,000	52,600	44,400	43,900	47,000
ACTUAL INST q''_{BOO}	78,000	74,000	74,000	58,000		61,000	65,000	76,000	52,600	44,400	43,900	47,000

Notes:
1. Valve position given in top line is rotation from full open of a flow-limiting plug cock in the downcomer.

2. Units are psia for pressure, 10^5 lbm/hr ft^2 for mass flow rate, and Btu/hr ft^2 for burnout heat flux.

3. Average values of oscillatory mass flow rates are given. All flows are oscillatory at burnout except those marked *.

4. Predicted burnout heat fluxes are calculated by the correlation of Tong, Currin, and Thorp, which is Equation (1) of Reference 15.

The burnout heat flux predicted by the correlation of Tong, Currin, Thorp (15) are also given in Table 1. Although this correlation was derived for high pressure water, the agreement is good for the cases where the flow is not oscillatory (columns indicated by asterisk). Where the flow is oscillatory, the average value of the flow is used in the correlation, and the agreement with experimental results is poor, occurring at a much lower heat flux than predicted. The agreement is poorest where the amplitude of the oscillation is the greatest, i.e. at low pressures with flow valve wide open.

Approximate values of maximum instantaneous heat flux at burnout as determined from the experimental measurements using Eq. (1) are also listed in Table 1, and fair agreement is noted with the burnout heat flux predicted using the average mass flow rate. The agreement is good enough to suggest that burnout occurs in oscillatory flow when the instantaneous heat flux, rather than average heat flux, reaches the value predicted by steady-flow correlations.

Void Fraction

Void fraction measurements for a system pressure of 75 psia are presented in Fig. 4. Contours of constant slip ratio determined from Eq. 3 are included. The relationship proposed by Bankoff (16), Eq. (4), is also plotted, taking the value of the flow parameter $K = 0.89$.

$$\alpha = \frac{Kx \cdot \rho_f/\rho_g}{1 + x(\frac{\rho_f}{\rho_g} - 1)} \tag{4}$$

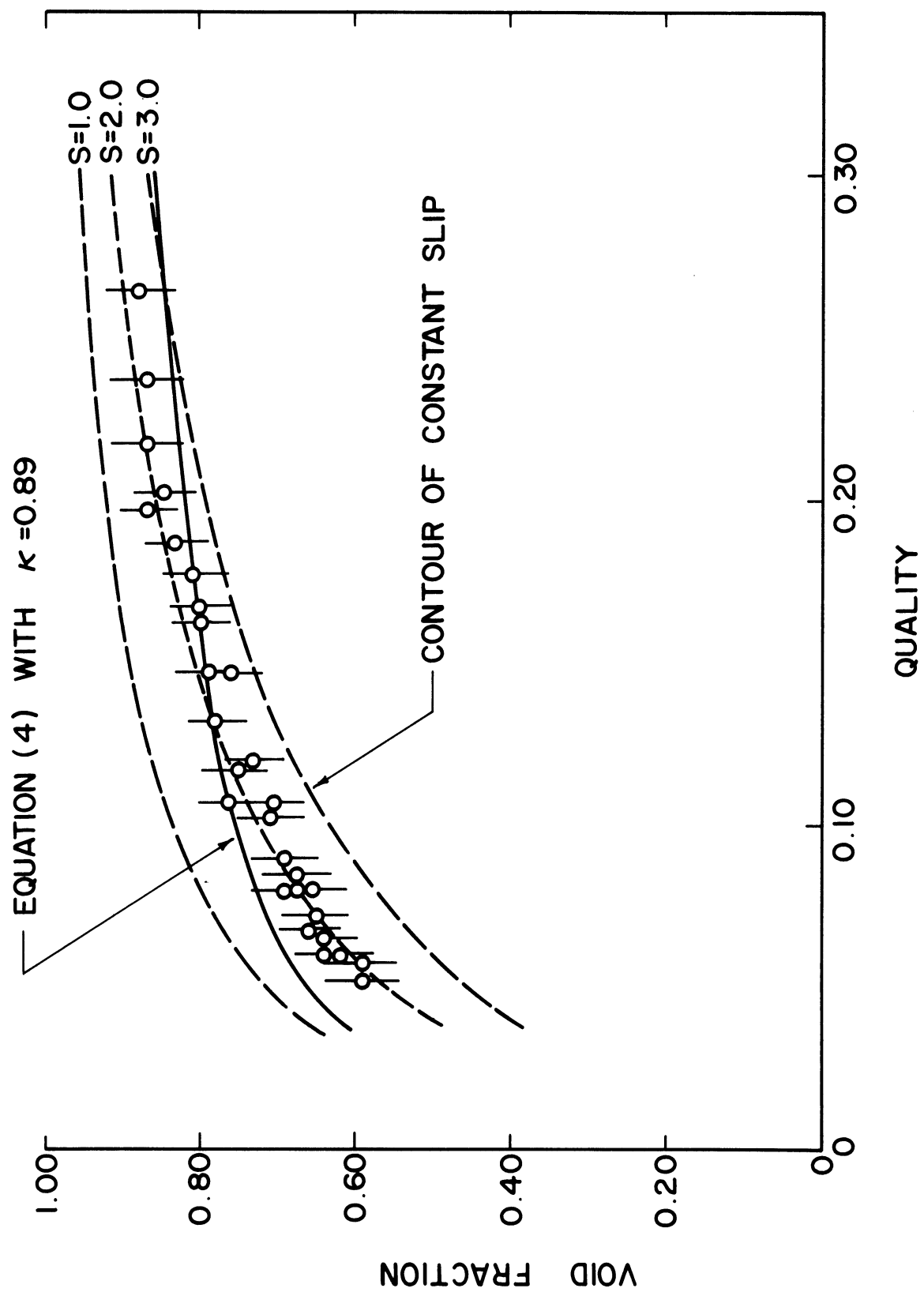Figure 4. Static Void Fraction at 75 Psia.

EFFECT OF CARRIAGE MOTION

Flow Surge Peaks, Flow Initially Steady

When the carriage is oscillated, the fluid in the natural circulation system surges in response to the periodically varying driving head. Fig. 5 presents typical data showing the ratio of the mass flow rate peaks as a function of the peak acceleration at several carriage frequencies. This ratio is almost linear with peak acceleration for any one frequency.

The dependence of the flow peak ratio on frequency, for a given value of a_{MAX}/g , is shown by cross-plotting Fig. 5. This is done in Fig. 6 for $a_{MAX}/g = 1.25$, using the points lying along this ordinate in Fig. 5, as well as additional similar data. Fig. 6 applies for wide open flow valve and 75 psia; Fig. 7 is similar, but for other flow valve positions. The zero-frequency terminus of each curve in Figs. 6 and 7 is the ratio of calculated mass flow rates at steady 1.25g, to that at 1.0g

A distinct resonance effect is noted in both figures, indicating a natural frequency for the system. This bears a resemblance to the resonance curves of elementary mechanical vibration theory, and the data can be well fitted for $\frac{\omega}{\omega_N} \leq \sqrt{2}$ by the transmissibility equation:

$$M = \frac{\sqrt{1 + (2\zeta \frac{\omega}{\omega_N})^2}}{\sqrt{[1 - (\frac{\omega}{\omega_N})^2]^2 + (2\zeta \frac{\omega}{\omega_N})^2}} \tag{5}$$

which expresses the transmissibility of a single degree of freedom machine foundation. As used here, M is the ratio of the peak mass flow rate,
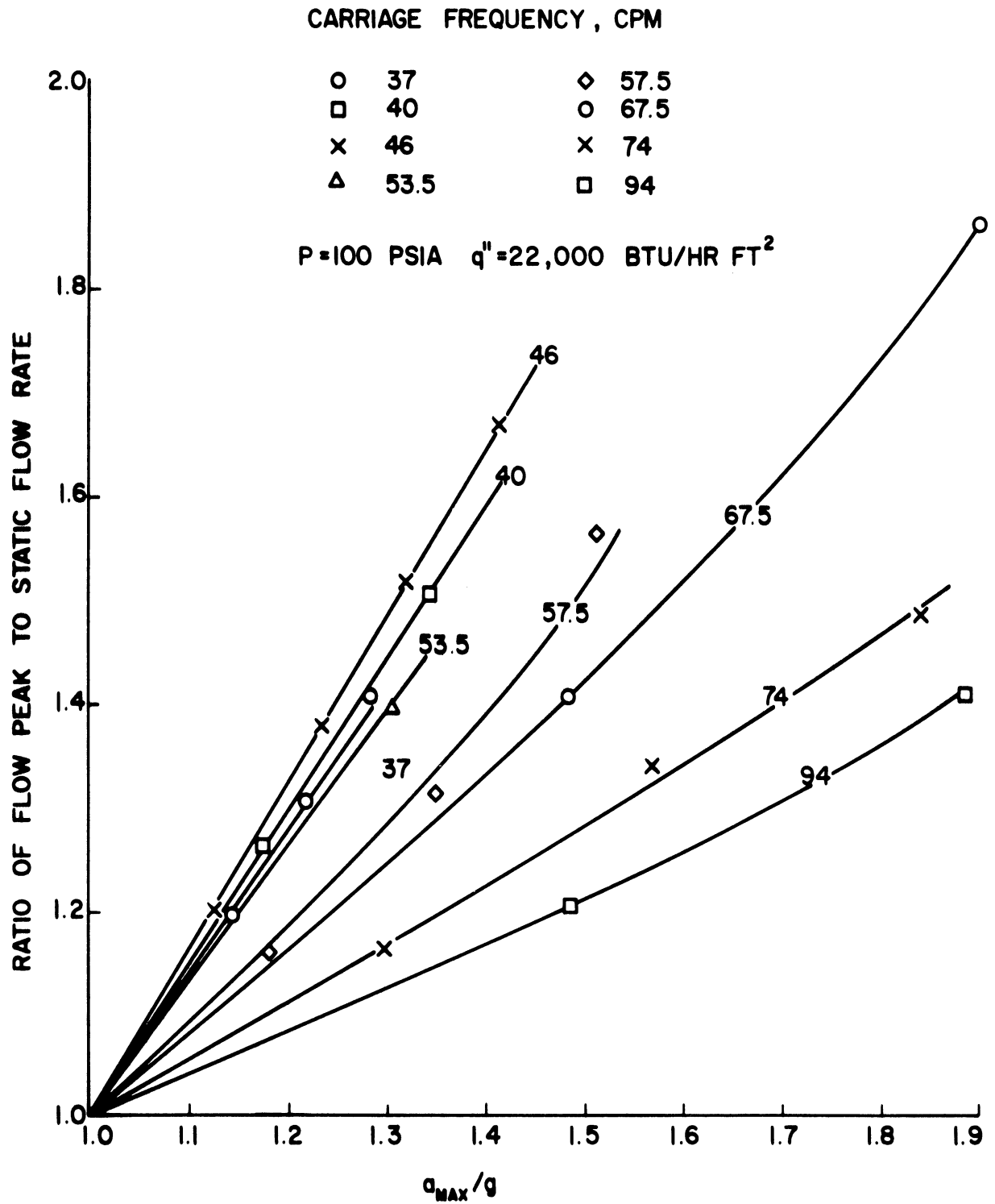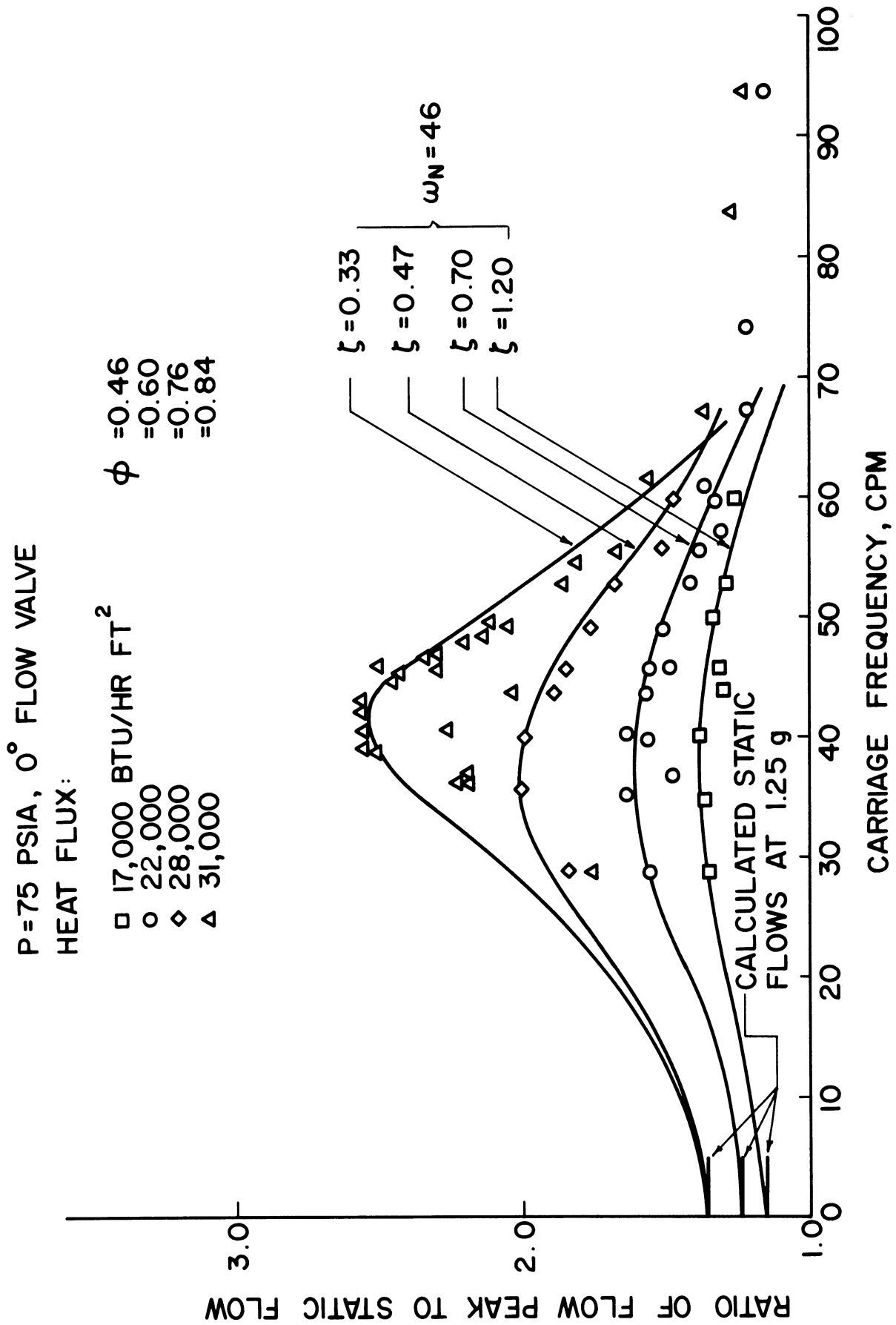
Figure 5. Flow Peak Data.

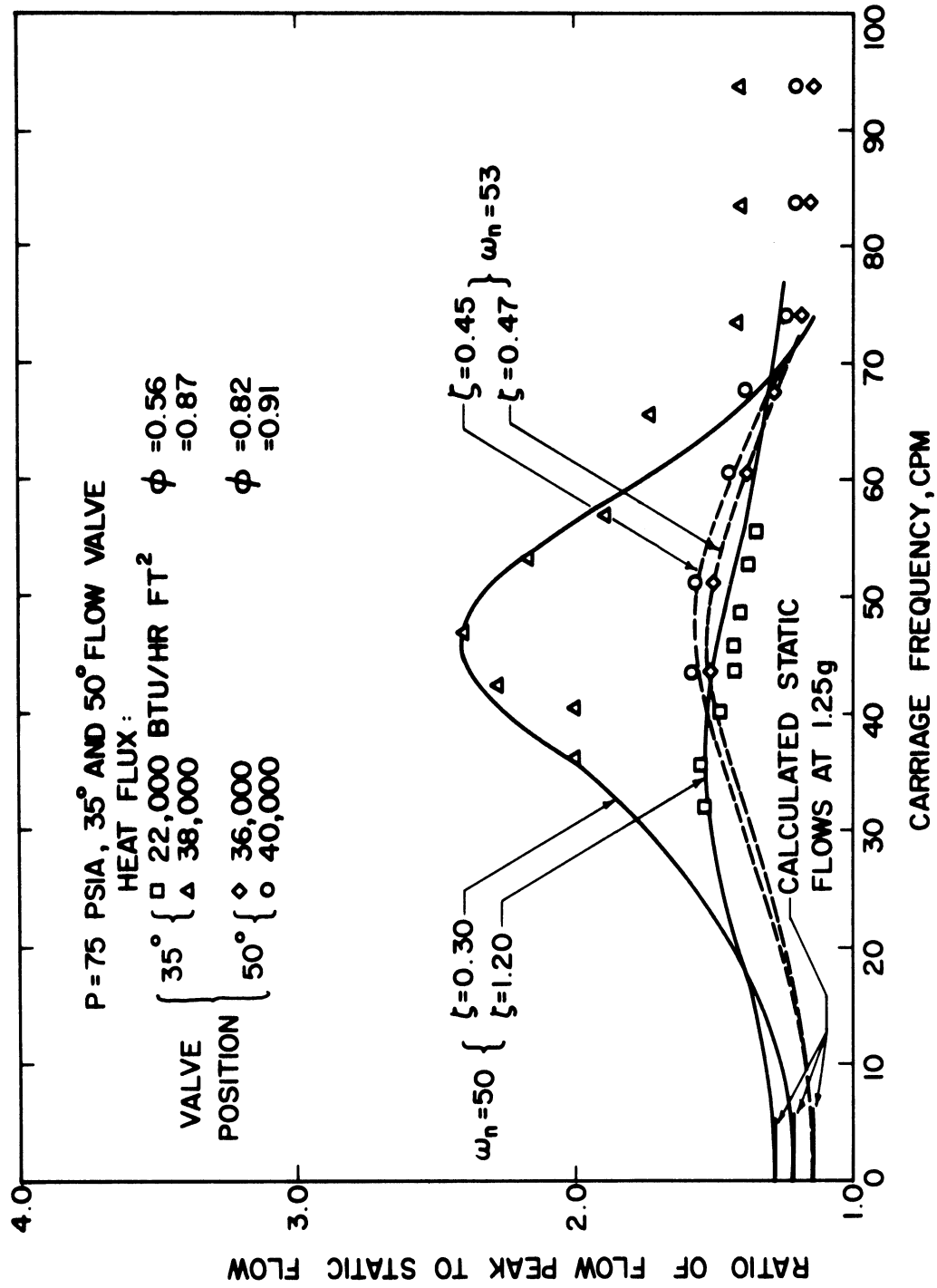Figure 6. Flow Peak Data at $a_{MAX} = 1.25$ g .

Figure 7. Flow Peak Data at $a_{MAX} = 1.25\ g$.

with carriage oscillating, to the calculated steady mass flow rate at a steady 1.25g. The curves in Figs. 6 and 7 are plots of this equation with a value of M chosen in each case to fit the data at the resonant peak.

Values of the damping ratio ζ are plotted in Fig. 8 as a function of the parameter ϕ, which is the ratio of heat flux to the heat flux at which flow oscillations begin (or the burnout heat flux for the 50° valve position). Points are included for system pressures of 50 and 100 psia, as well as the 75 psia data from Figs. 6 and 7. The data indicate that ζ is a function of ϕ only, being essentially independent of system pressure and flow valve position. Similar results would be found at other values of a_{MAX}/g, since the peak amplitude is almost a linear function of this parameter, as indicated by Fig. 5, and a functional dependency could be found, giving

$$\zeta = f_1(\phi, a_{MAX}/g) \tag{6}$$

Substituted into Eq. (5), then

$$M = f_2(\frac{\omega}{\omega_N}, \phi, a_{MAX}/g) \tag{7}$$

For a system operating at specified values of heat flux, a_{MAX}/g, and forcing frequency ω, M can be computed, and thus the peak mass flow rate determined.
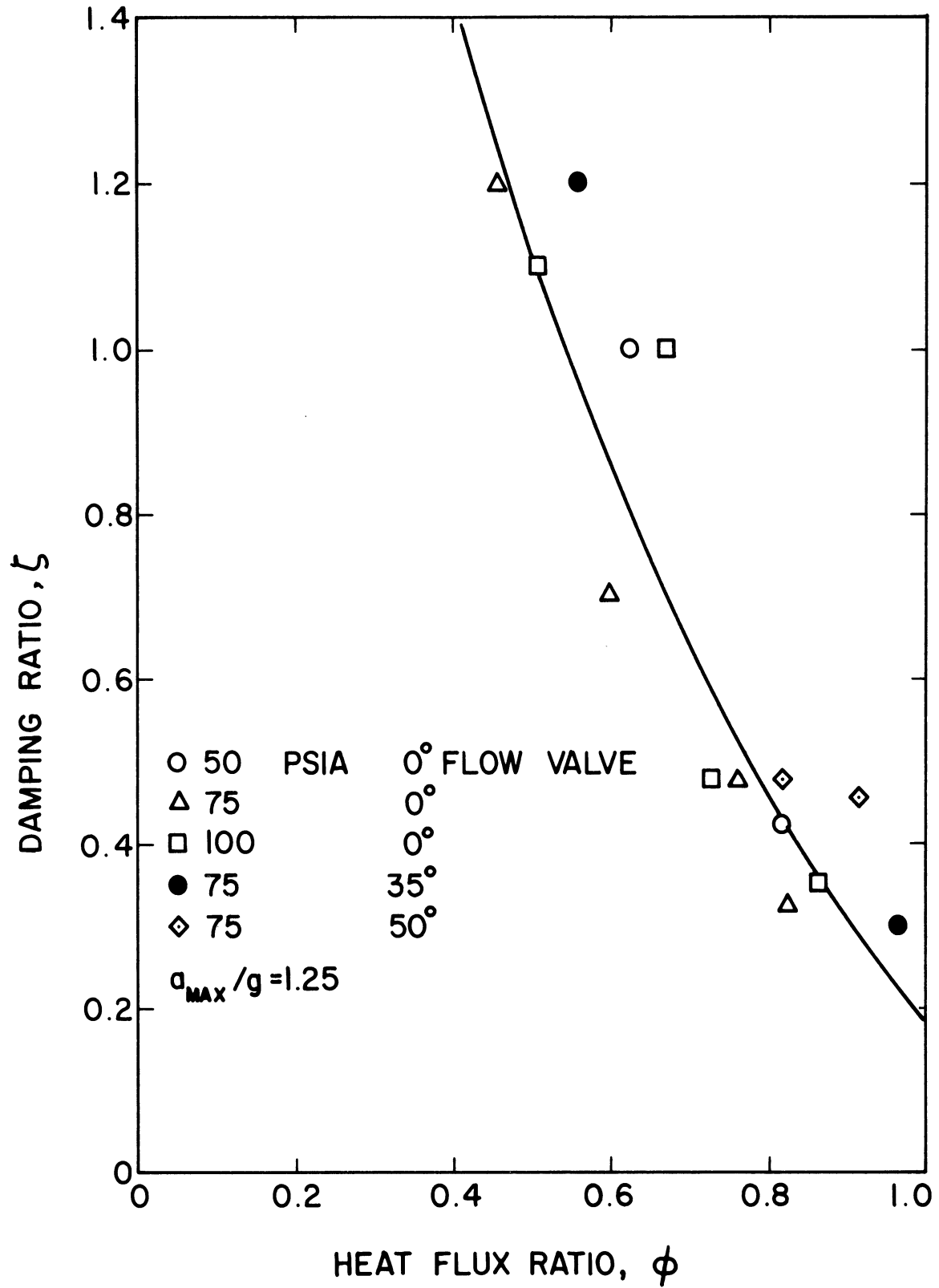
Figure 8. Damping Ratio Correlation.

Flow Surge Peaks, Flow Initially Oscillating

The results of imposing carriage motion on naturally oscillating flow are more complex than in the case of naturally steady flow. Three principal areas of differing qualitative behavior can be identified in the data taken here:

1) If the frequency of the carriage oscillation is much lower (approximately 10 cpm or more) than the natural frequency, then both oscillations are present in the mass flow rate signal.

2) If the frequency of the carriage oscillation is much higher (again approximately 10 cpm or more) than the natural frequency, both forced and natural frequencies also appear in the mass flow rate signal. An example is shown in Fig. 9. Two quantitative differences exist between this behavior and that of (1). First, the high frequency carriage oscillation amplitude, while the low frequency carriage oscillation does not. Second, the highest peaks, which periodically occur when forced and natural driving heads coincide, are much higher in this case because of the higher peak accelerations.

3) If forced and natural frequencies are nearly the same, then the mass flow rate oscillates at the forced frequency only. The frequency range for which this occurs is referred to as the resonance region. The amplitude of the mass flow rate peak is greater than in the natural oscillation condition existing before motion starts, and is a maximum when forced and natural frequencies coincide. However, as forcing frequency is raised above natural frequency, the peak flow rate amplitude may decrease below the natural amplitude before the frequency
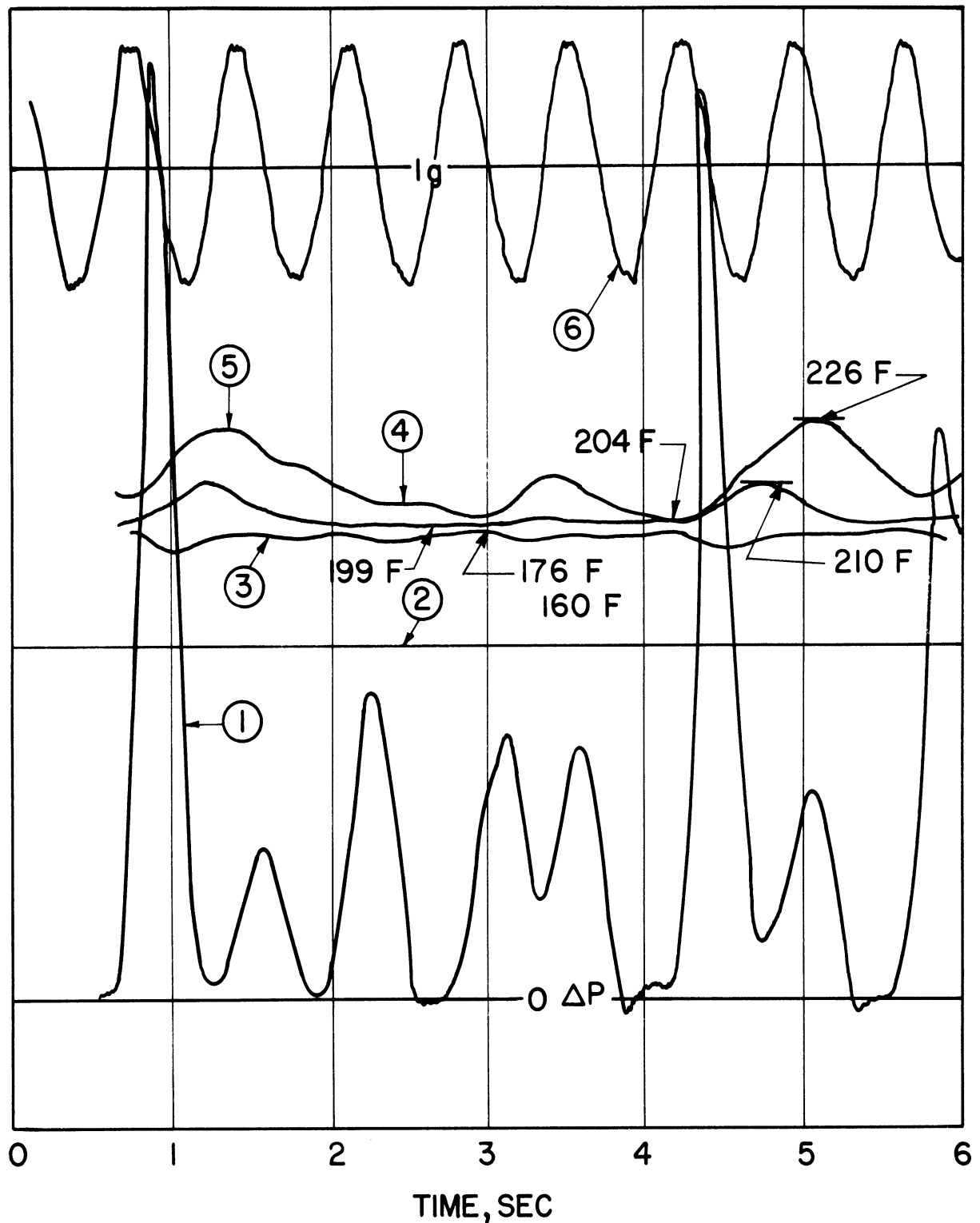
Figure 9. Recorder Chart of Flow and Temperature, Combined
Natural Oscillation and Carriage Motion.

corresponding to behavior (2) is reached. This phenomenon occurs con-
sistently in the neighborhood of 68 cpm when the flow valve is wide open,
but no explanation for it has been developed. It is significant because
of the associated increase in burnout heat flux, which contrasts with the
decrease due to motion experienced generally at other frequencies.

The carriage frequency at which the transition between the
three areas of behavior occurs depends on the relative magnitudes of
forced and natural driving heads. For example, the longer the carriage
stroke, the wider the band of frequencies over which carriage frequency
alonge appears in the flow signal. Conversely, raising the heat flux,
which increases the natural driving head, causes the natural oscillation
to appear at carriage frequencies closer to the natural frequency.

System Performance

Since the rate of heat generation within the tube walls is
held constant, the average vapor generation rate is constant and inde-
pendent of carriage motion.

Net mass flow rate during carriage motion is difficult to
determine with accuracy in the cases where flow reverses during part
of the motion cycle. When flow does not reverse, as with the lower
a_{MAX}/g , or with the flow valve attenuating the peaks, integration of
the instantaneous mass flow rates shows no significant change caused
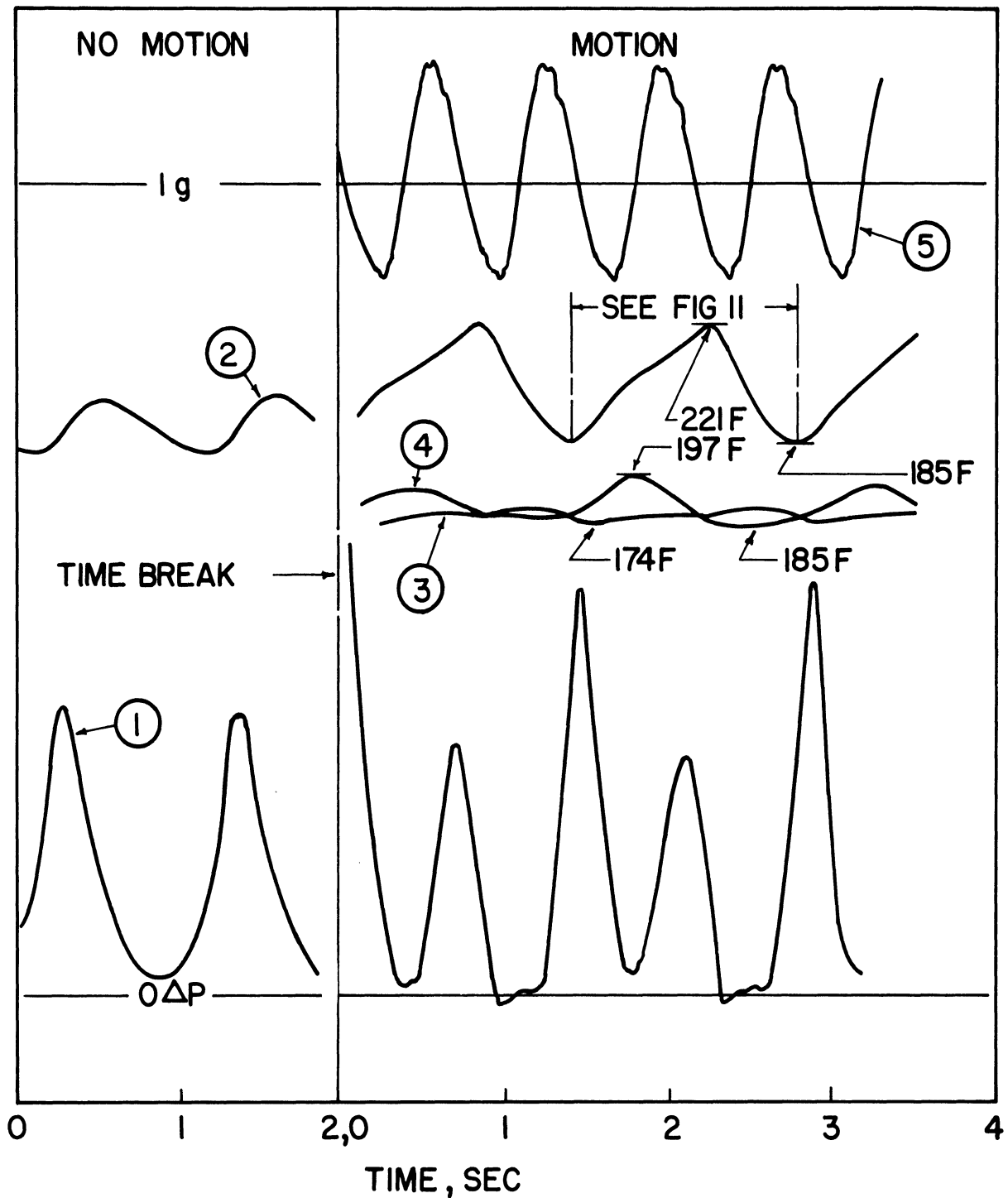by the carriage motion.

Tube Wall Surface Temperatures

Flow oscillations cause oscillations in wall temperature of
the heated tube. A recorder trace of outer surface temperature is given

in Fig. 10, and the calculated transient component of the inner surface temperature and the heat flux over a single cycle are given in Fig. 11. A possible cause for wall temperature oscillations of this magnitude is the periodic transition to film boiling during the low-flow part of the flow cycle. The evidence for this conclusion is the rate of temperature rise of the wall, which is almost equal to that calculated when no heat is being removed from the wall, indicating that the inner surface is vapor bound. The time average heat flux in Fig. 11 is approximately 90 percent of the static burnout flux.

Burnout

Under some conditions, motion of the carriage is found to cause burnout at an average heat flux lower than the static value. A recorder chart showing burnout occurring because of carriage motion is reproduced in Fig. 12. Data is presented in Figs. 13-15 for a system pressure of 75 psia, and flow valve positions of 0, 35, and 50 degrees, respectively. Results at pressures of 50 and 100 psia are quite similar.

The data 0° and 35° valve positions (Figs. 13 and 14) show the resonance effect. The decrease in burnout heat flux is greatest in the neighborhood of the natural flow oscillation frequency. With the flow valve position of 50° (Fig. 15), no resonance effect is present, and the decrease in burnout heat flux is nearly the same for all frequencies tested. The difference is that natural flow oscillation occurs before burnout for 0° and 35° valve positions, while it does not for the 50° position.

Figure 10. Recorder Chart of Flow and Temperature, Combined Natural Oscillation and Carriage Motion.
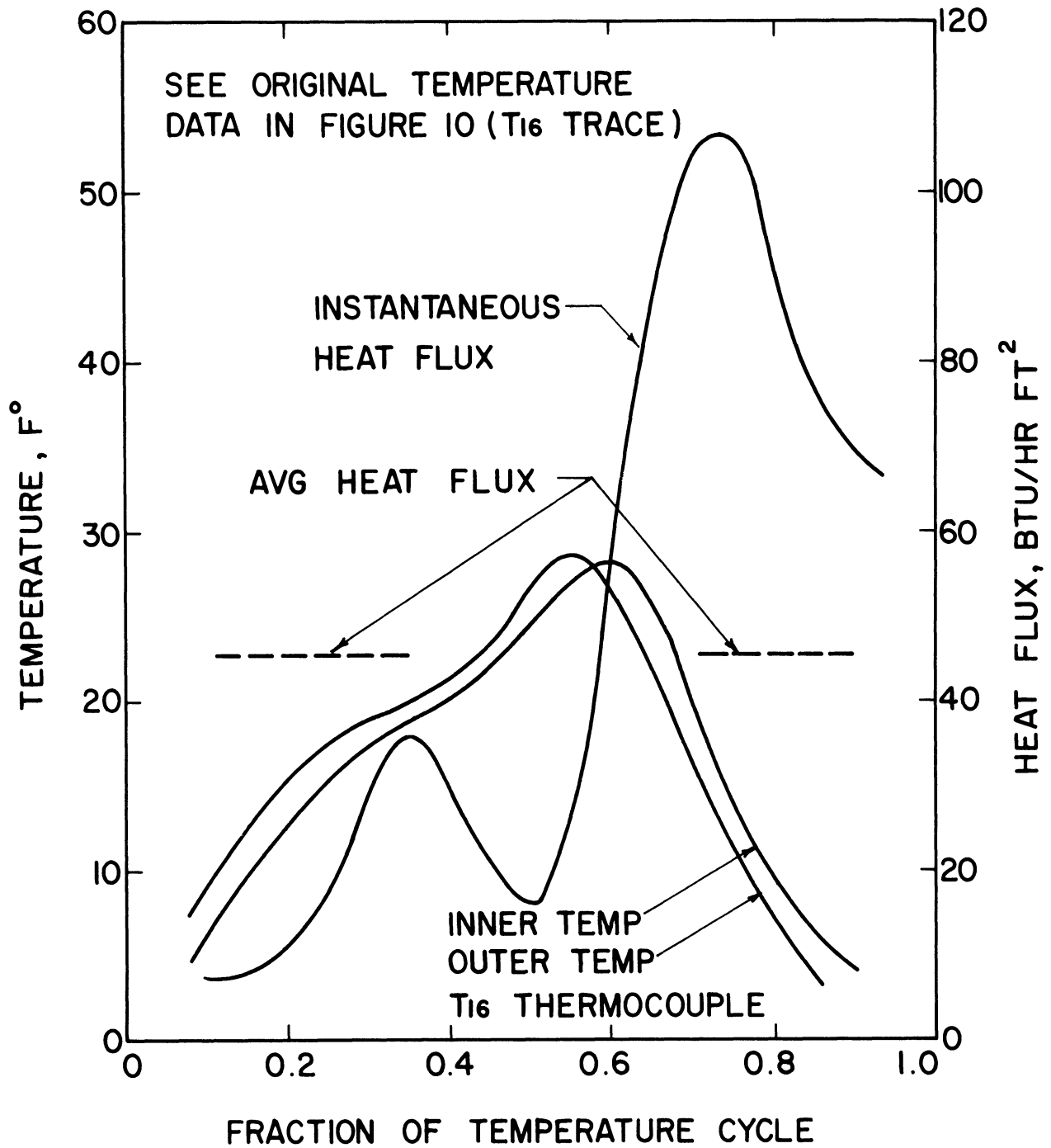
Figure 11. Transient Components of Inner and Outer Tube Wall
Surface Temperatures and Inner Surface Heat Flux.
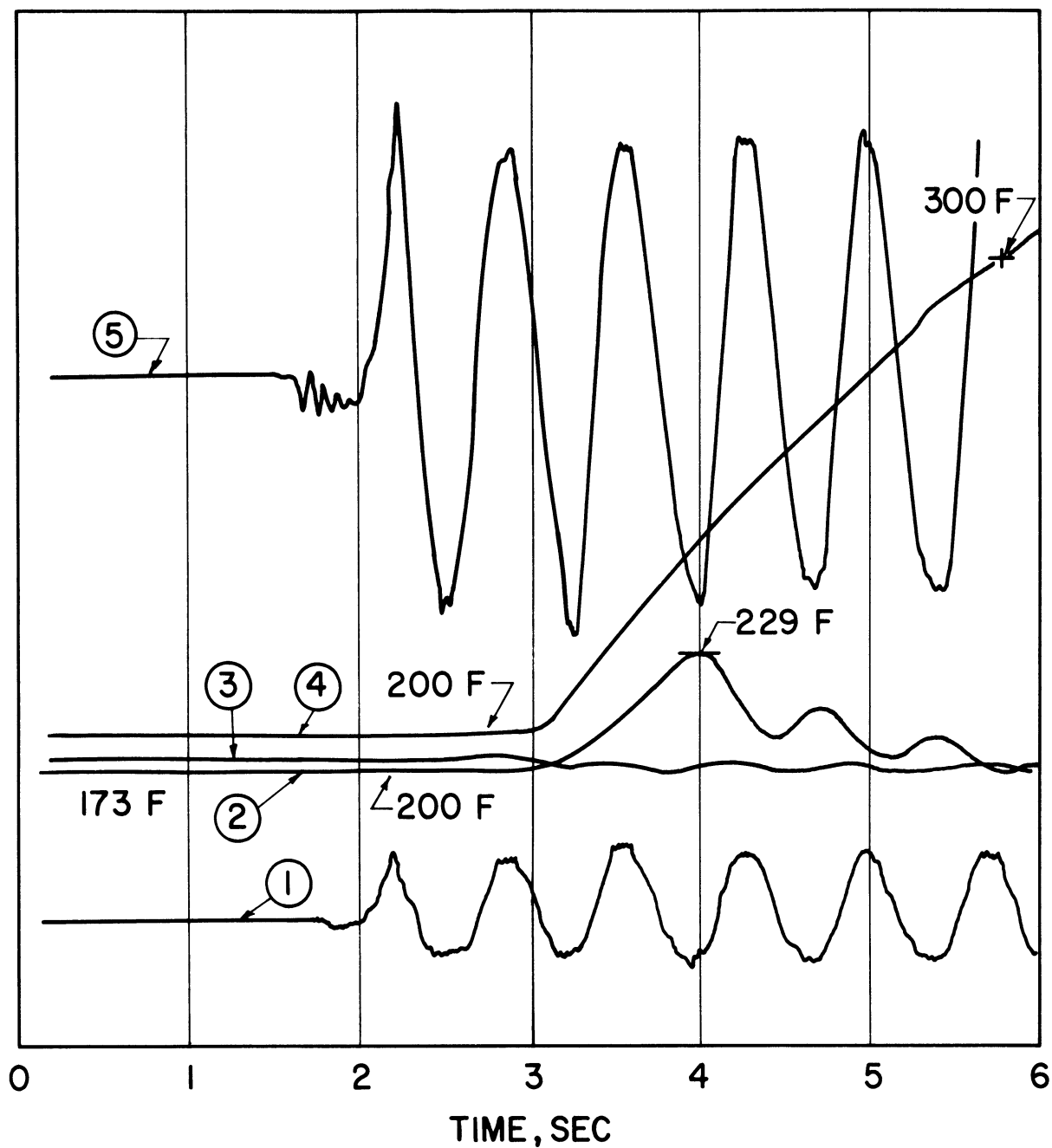
Figure 12. Recorder Chart Showing Burnout Occurring After Start of Carriage Motion.
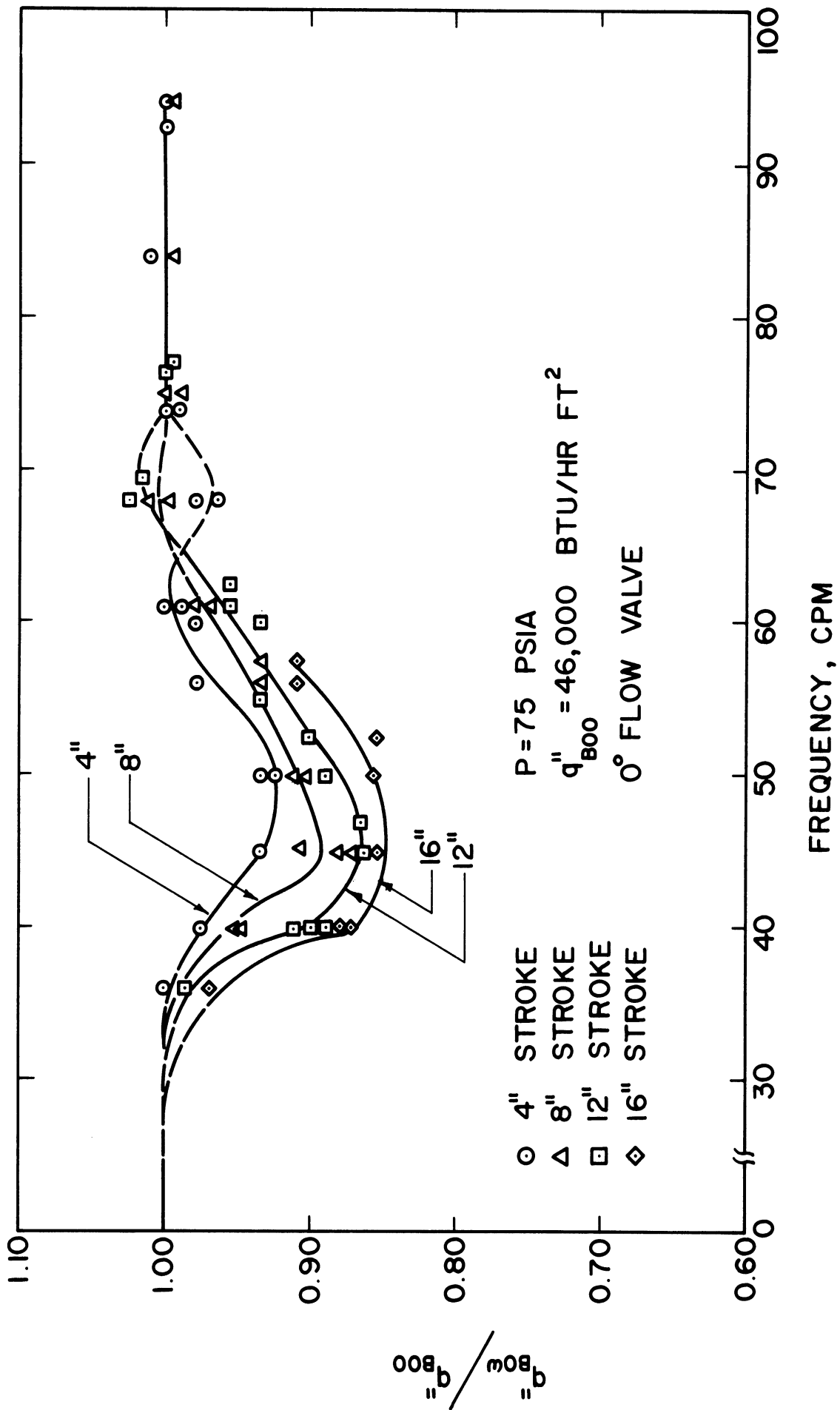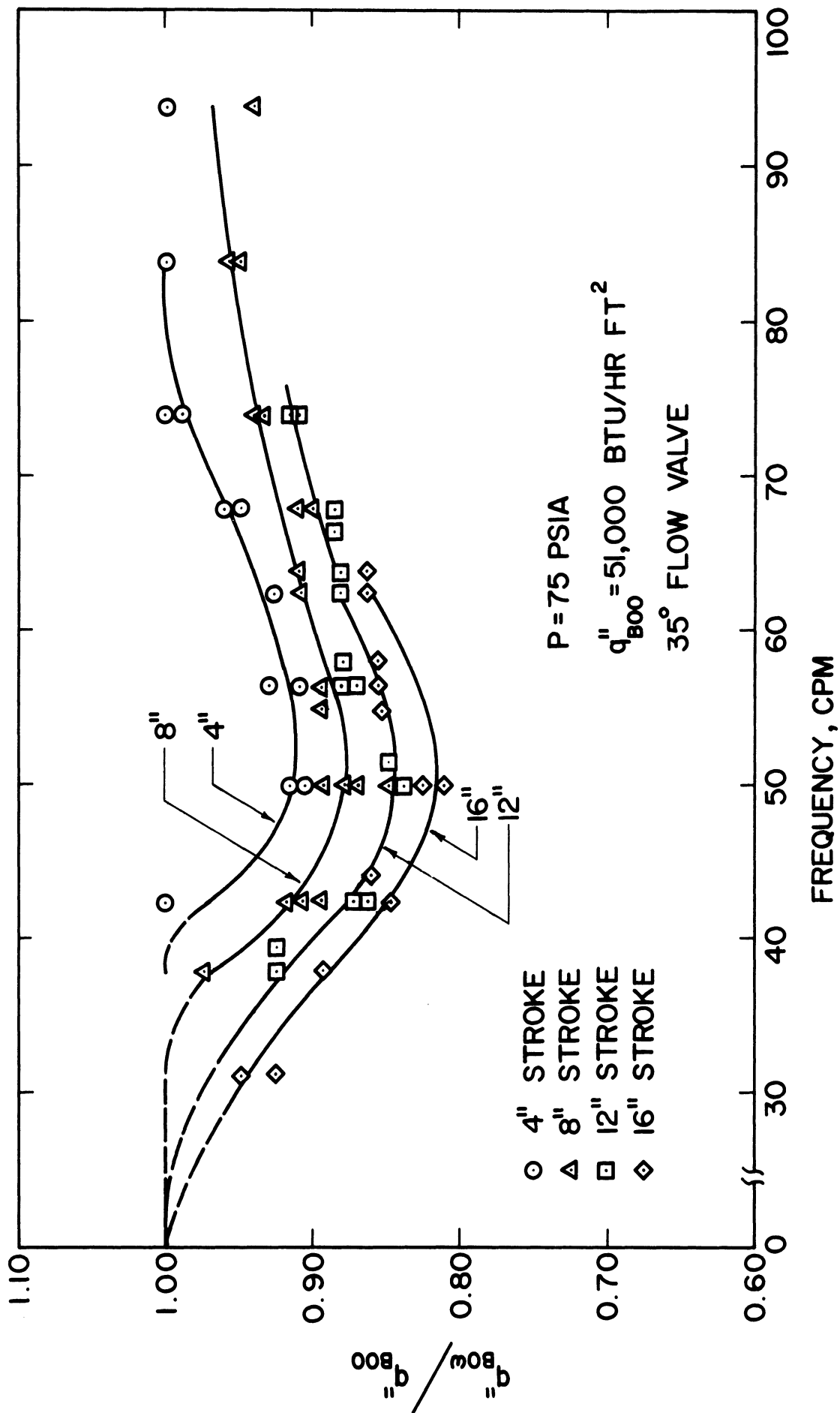
Figure 13. Burnout with Carriage Motion.
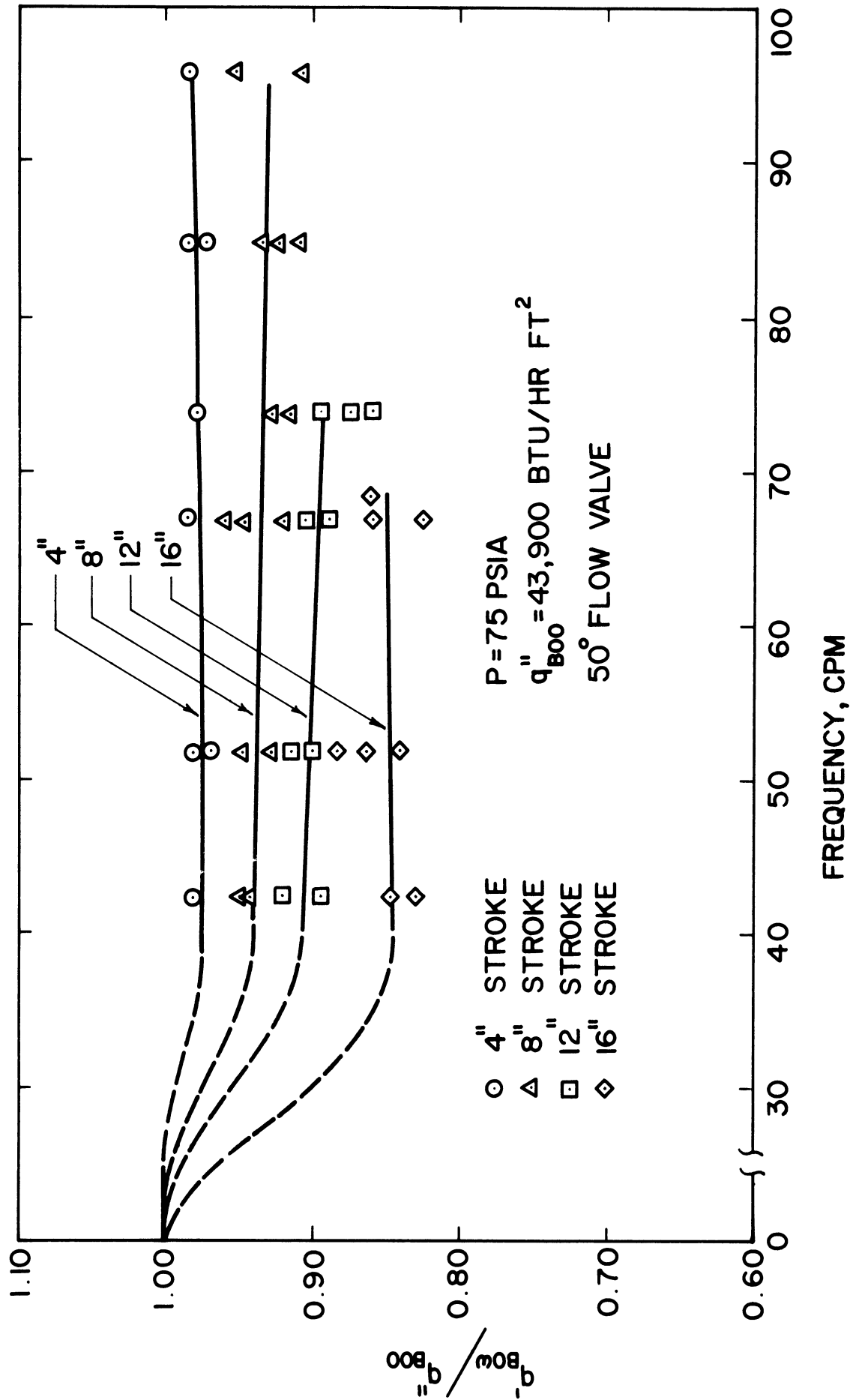
Figure 14. Burnout with Carriage Motion.

Figure 15. Burnout with Carriage Motion.

The explanation lies in the sequence of events in oscillatory flow burnout, which is postulated to follow these steps:

1) As the amplitude of flow oscillation is increased, either by increasing heat flux or by increasing carriage motion, a point is reached at which nucleate boiling ceases during part of the low-flow portion of the cycle. During this interval, the surface is film bound, and wall temperature rises rapidly. When the film is disrupted by increasing liquid flow, the wall temperature drops rapidly.

2) As the flow oscillation amplitude is increased further, from either cause, the vapor-bound condition exists over a longer interval, so that the wall temperature rises higher before nucleate boiling is restored.

3) As the flow oscillation amplitude is increased still further, from either cause, the wall temperature rises to a sufficiently high level during the vapor-bound interval that it is not reduced to its original level during the remainder of the flow cycle. As a result, temperature rises higher each cycle until nucleate boiling can no longer be restored. Film boiling exists permanently, and wall temperature rises continuously to a level consistent with this boiling regime.

It is then apparent that increasing the amplitude of flow oscillation reduces the burnout heat flux, since increased amplitude results in a longer interval of vapor binding. When there is resonance between natural and motion-forced oscillation, amplitudes are higher than without motion, and so burnout flux levels are reduced. When the flow

valve is closed enough to suppress all natural oscillation, carriage motion at any frequency causes periodic flow peaks of higher than natural (i.e. zero) amplitude, hence significant decrease in the burnout heat flux occurs at all frequencies.

Except for the highly restricted 50° valve position, there is reason for expecting high frequency motion to raise the burnout heat flux above the level obtained with no motion, since when $\omega \gg \omega_N$, the combined forced and natural oscillation flow peaks are generally lower than natural oscillation flow peaks alone. In view of the preceding discussion, lower values of flow rate peaks should raise the burnout heat flux. However, the burnout data, with an exception discussed in the next paragraph, does not show a significant increase in burnout heat flux. The explanation for the paradox lies in the exceptionally high flow peaks which occur when the natural and forced driving heads momentarily coincide. When the heat flux is near the static burnout level, a single abnormally low-flow interval will be sufficient to establish an unbreakable vapor film.

As discussed earlier, a narrow range of carriage frequencies exists at the upper end of the resonance region in which the flow peak amplitude is less than the natural oscillation amplitude. The effect of this phenomenon can be seen in the burnout data of Fig. 13, wherein burnout heat flux is slightly higher at 68 cmp, 8 and 16 inch stroke lengths than the static value. The flow peak measurements taken with the burnout data show that the mass flow peaks are uniform in height, and consistently lower than the natural peaks with the carriage stationary.

The discussion above relates the change in the burnout heat flux due to carriage motion to the oscillation of the mass flow rate, along with the rise in wall temperature occurring during the low-flow part of the cycle. This latter phenomenon suggests that the burnout heat flux may depend on the heater tube properties, as well as on the frequency and amplitude of the imposed flow oscillation. The parameter $[\omega/2\kappa]^{1/2}\delta$ arises as the argument of the functions which comprise the solution of the heat diffusion equation with a sinusoidal boundary condition, and appears to be a reasonable selection to correlate these effects. Fig. 16 is a plot of $R_{\dot{m}}/[\frac{\omega}{2\kappa}]^{1/2}\delta$ versus $q''_{BO\omega}/q''_{BOO}$, where $R_{\dot{m}}$ is the ratio of the peak mass flow rate at burnout with carriage in motion to the peak mass flow rate at burnout with carriage stationary. The results tend to support the hypothesis that burnout with motion is a function of the peak (or minimum) mass flow rate and the time during which the minimum flow rate exists.

Void Fraction

Void fraction measurements made at 50 psia, 0° valve position, are presented in Fig. 17 for three values of heat flux. This is typical of data taken for 50, 75 and 100 psia, over the frequency range from 40 to 60 cpm, and indicates a cyclic variation in void fraction.

The void fraction readings are made by counting over a number of successive gate times, each constituting approximately 1/8 of the carriage motion cycle. Each data point consequently represents an average over this interval and over the same interval of successive cycles.
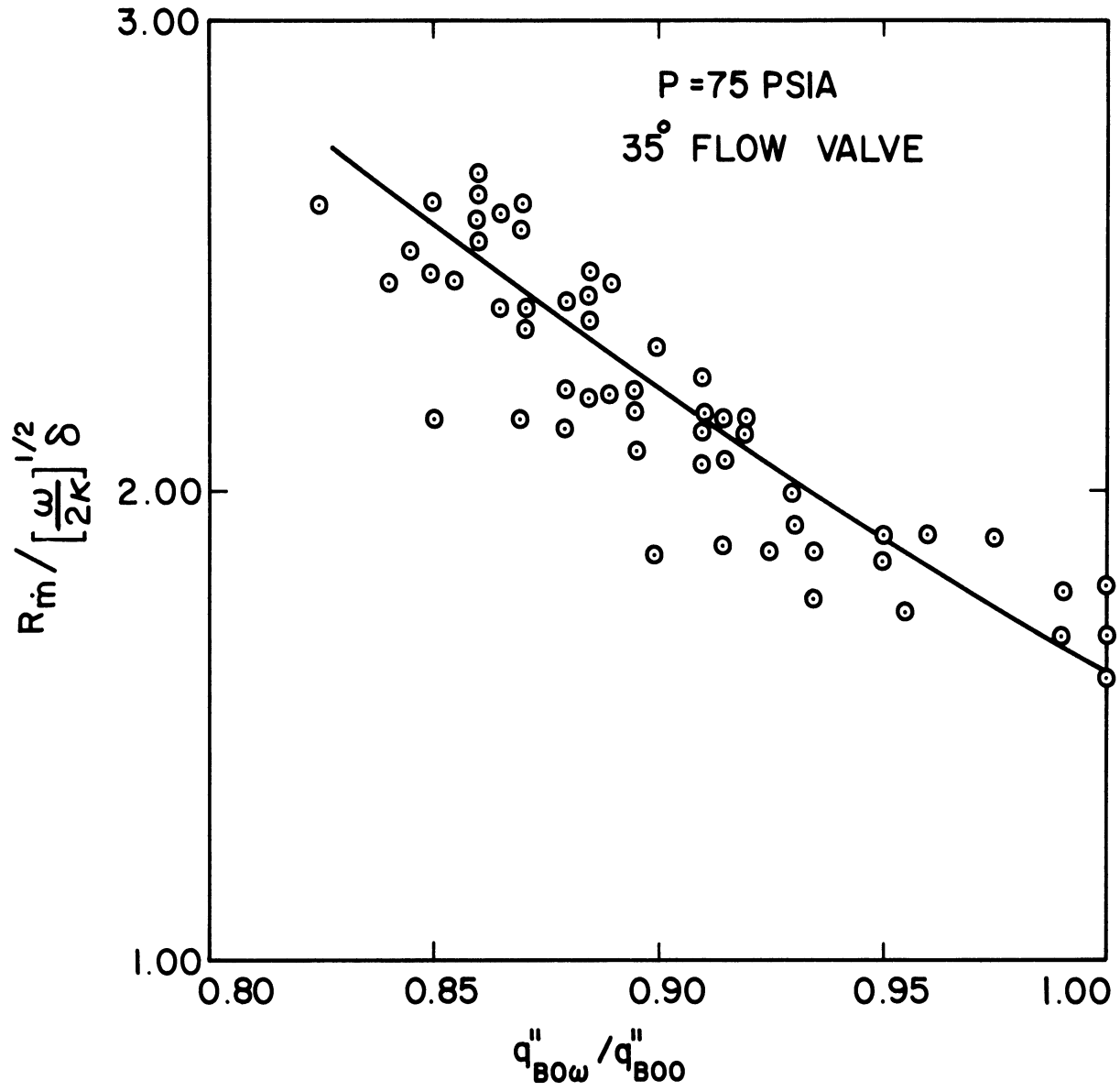
Figure 16. Burnout Flow Peak Correlation.

PRESSURE 50 PSIA

o X =0.08 , q"=17,500 BTU/HR FT^2

△ X =0.11 , q"=20,000

□ X =0.19 , q"=24,800

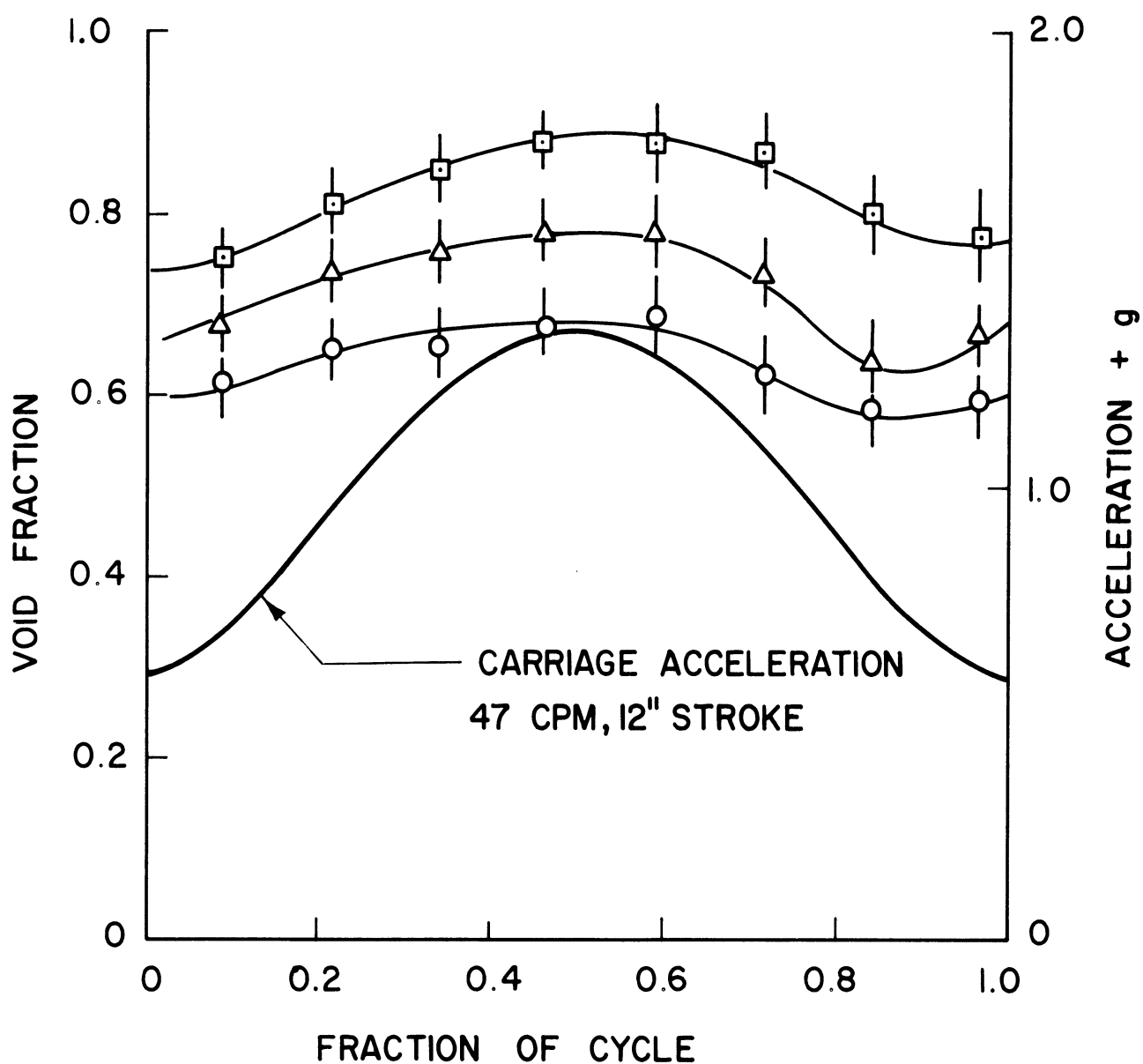GATE TIME =0.15 SEC/CYCLE

Figure 17. Void Fraction with Motion.

The effect of carriage acceleration, also plotted, is evident
in Fig. 17. For example, the dip which occurs near the right edge
results from the surge of low-quality fluid that passes the point of
measurement 0.3 to 0.4 of the cycle after maximum carriage acceleration.

The data for Fig. 17 is taken by the "one shot" method, i.e.
a single reading along the tube diameter. The data is corrected before
plotting by a factor which relates average void fractions to one-shot
data as a function of quality. This correction was discussed earlier
with reference to void fraction measurements with the carriage stationary.
Use of the static correction factor may introduce an error, since
quality will vary from the static value during various parts of the
cycle. The magnitude of the error was explored by making one set of
readings with the densitometer being traversed so that an actual average
void fraction would be found at each point. The results are indicated
in Fig. 18, wherein the data for $q'' = 20,000$ from Fig. 17 is repeated
(labelled "corrected"), along with the uncorrected one shot data and the
data taken by traversing. Differences between data obtained by the
"one shot" corrected method and the traversing method are evident at
points where extremes of high or low quality occur, but the differences
are not greater than the uncertainty intervals indicated in Fig. 17.

PRESSURE 50 PSIA

$X = 0.11$, $q'' = 20,000$ BTU/HR FT^2

GATE TIME 0.15 SEC/CYCLE

⊙ ONE SHOT DATA, UNCORRECTED
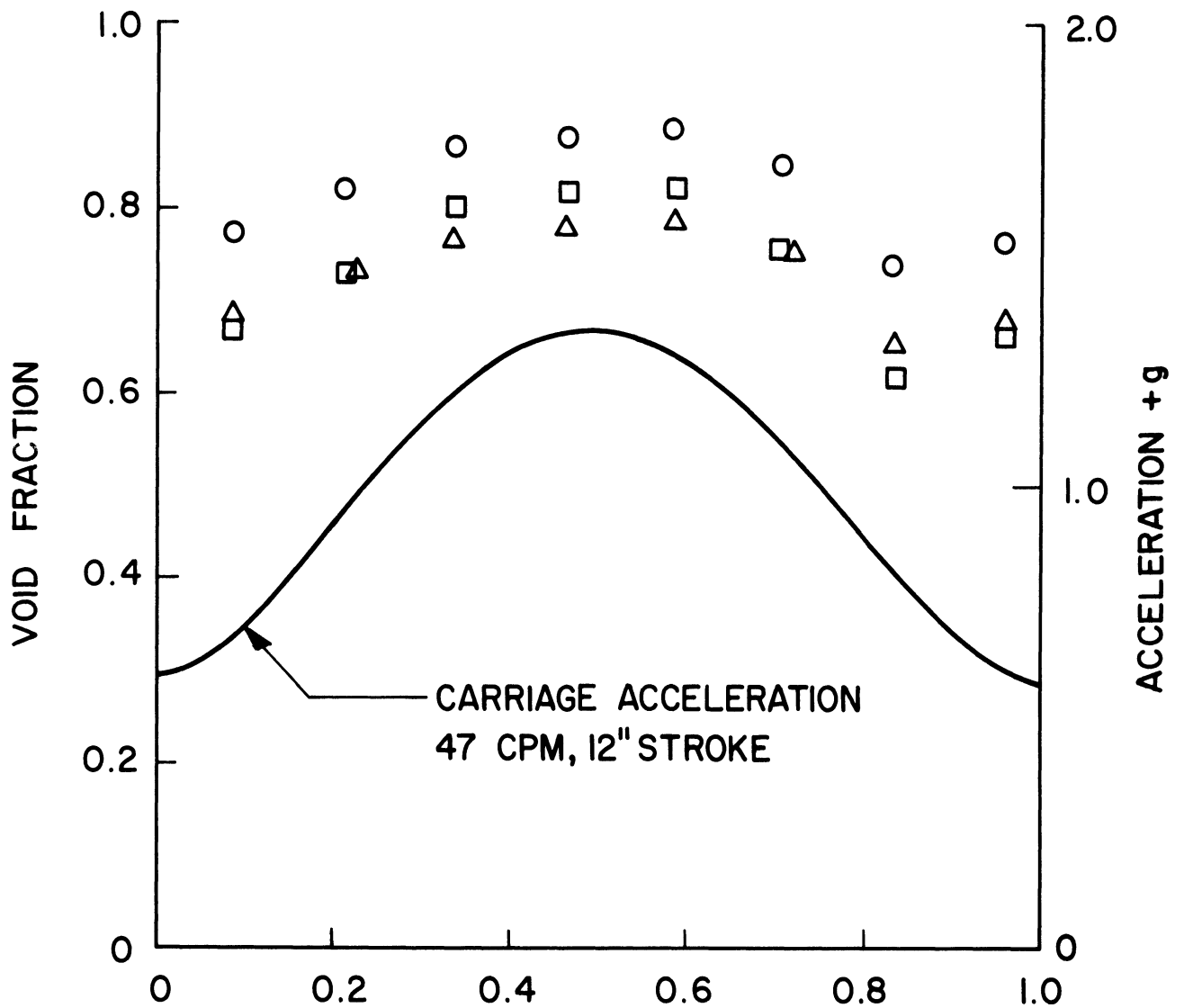△ ONE SHOT DATA, CORRECTED
□ DATA TAKEN BY TRAVERSING
DENSITOMETER

Figure 18. Void Fraction with Motion - Comparison
of Methods.

CONCLUSIONS

Over the range of acceleration, frequencies, system pressures, and subcooling used in this program, the following conclusions can be made:

1) If the static flow is steady, then carriage motion causes mass flow rate oscillations whose amplitudes are a linear function of a_{MAX}/g , for any frequency. As a function of frequency, these amplitudes show a resonance with system natural frequency. The amplitudes are also functions of a damping ratio, which in term is a function only of the parameter ϕ .

2) If the static flow is oscillatory, the effect of system oscillatory motion is more complex, but the general tendency is an increase in mass flow rate peak amplitude when the natural and forcing frequencies are nearly the same, and no increase, at least in average peak amplitude, otherwise.

3) Average mass flow rate is not significantly affected by system oscillatory motion.

4) Burnout heat flux is reduced by motion whenever the motion increases the average flow peak amplitudes above their static value. In this case wall temperature data indicates that an interval of film boiling occurs during a part of the cycle, at average values of heat flux below the burnout heat flux.

5) Vapor void fraction varies in response to the carriage motion. It appears that the variation is no more than that expected from variations in quality due to unsteady flow.

LIST OF REFERENCES

1. Quinn, E.P., and Case, J. M., "Natural Circulation Loop Performance at 1000 Psia under Periodic Accelerations," AEC Report GEAP-3397 (Rev. 1), 1960.

2. Quinn, E.P., "Further Experimental Results on Natural Circulation Loop Performance at 1000 Psia under Periodic Accelerations," AEC Report GEAP-3397 (addendum), 1960.

3. Kjelland-Fosterud, E., Bencze, I., Kierulf, B., and Kolberg, O.R., "Two-Phase Flow Investigation for a Marine Boiling Water Reactor," A/Conf 28/P/801 Third United Nations International Conference on the Peaceful Uses of Atomic Energy, May 1964.

4. Isshike, N., "Study of the Effects of Heaving and Listing on Thermal and Hydraulic Performance of Water Cooled Marine Reactors," Journal of the Japan Society of Mechanical Engineers, Vol. 68, page 28, 1965 (in Japanese).

5. Hooker, H. H., and Popper, G. F., "A Gamma Ray Attenuation Method for Void Fraction Measurement in Steam-Water Mixtures," AEC Report ANL-5766, 1958.

6. Petrick, M., "Investigation of Two-Phase Air-Water Flow Phenomena," AEC Report ANL-5877, 1958.

7. Egen, R.A., Dingee, D. A., and Chastain, J. W., "Vapor Formation and Behavior in Boiling Heat Transfer," AEC Report BMI-1163 (1957).

8. Woodward, J. B., "Natural Circulation Experiments in an Oscillating Force Field," PhD Thesis, University of Michigan, 1965.

9. Smith, W., Atkinson, G.L., and Hammitt, F. G., "Void Fraction Measurements in a Cavitating Venturi," Journal of Basic Engineering, Transactions ASME, Series D, Vol. 86, page 265, 1964.

10. Levy, S., and Beckjord, E.S., "Hydraulic Instability in a Natural Circulation Loop with Net Steam Generation at 1000 Psia," ASME Paper 60-HT-27, ASME-AIChE Heat Transfer Conference, Buffalo, 1960.

11. Mendler, O. J., Rathbun, A.S., Van Huff, N. E., and Weiss, A., "Natural Circulation Tests with Water at 800 to 2000 Psia under Nonboiling, Local Boiling, and Bulk Boiling Conditions," Journal of Heat Transfer, Transactions ASME, Series C, Vol. 83, page 261, 1961.

12. Wallis, G. B., and Heasley, J. H., "Oscillations in Two-Phase Flow
     System," _Journal of Heat Transfer,_ Transactions ASME Series C, Vol.83,
     page 363, 1961.

13. Jones, A. B., "Hydrodynamic Stability of a Boiling Channel," AEC
     Report KAPL-2170, 1960.

14. Meyer, J. E., and Rose, R. P., "Application of a Momentum Integral
     Model to the Study of Parallel Channel Boiling Flow Oscillations,"
     Journal of Heat Transfer, Transactions ASME, Series C, Vol. 85,
     page 1, 1963.

15. Tong, L. S., Currin, H. B., and Thorp, A. G., "New Correlations
     Predict DNB Conditions," _Nucleonics,_ Vol. 21, 5, 1963.

16. Bankoff, S. G., "A Variable Density Single Fluid Model for Two-Phase
     Flow," _Journal of Heat Transfer,_ Transactions ASME, Series C, Vol. 82,
     page 265, 1960.

LIST OF SYMBOLS

a sum of carriage acceleration and g, ft/sec^2

a_{MAX} value of a at carriage bottom dead center, ft/sec^2

C counts recorded by densitometer

C_f densitometer counts with $\alpha = 0$

C_g densitometer counts with $\alpha = 1$

C_m specific heat of tube wall, $Btu/lbm\ °F$

D inside diameter of heater tube, ft

F_c valve flow coefficient, gpm/1.0 psi

g acceleration of gravity, ft/sec^2

K flow parameter (in Eq. (4))

L length of heater tube, ft

M ratio, peak $\dot{m}$ with carriage in motion to steady mass flow rate at steady a/g equal to a_{MAX}/g .

$\dot{m}$ mass flow rate, lbm/hr

$\dot{m}_{AVG}$ average value of oscillatory $\dot{m}$, lbm/hr

P pressure, lbf/in^2

P_r reduced pressure

$R_{\dot{m}}$ ratio, peak in at burnout with carriage in motion to the peak in at burnout with the carriage stationary.

q'' surface heat flux, $Btu/hr\ ft^2$

q''_N time averaged value of heat flux, $Btu/hr\ ft^2$

q''_{BOO} value of q''_N at burnout with no motion, $Btu/hr,\ ft^2$

$q''_{BO\omega}$ value of q''_N at burnout with motion of carriage, $Btu/hr\ ft^2$

S   ratio of mean vapor velocity to mean liquid velocity

T temperature, °F

T_m temperature of tube wall, °F

T_{16}, T_{14} etc.   tube surface temperature at location designated, °F

               (thermocouples are located at 2 inch intervals on the

               tube outer surface, and are numbered from 1 nearest

               inlet to 16 nearest exit.)

t time, sec

x vapor quality

α vapor void fraction

δ thickness of tube wall, ft

ζ damping ratio, (Eq. (5))

κ thermal diffusivity, $\mathrm{ft}^2/\mathrm{sec}$

ρ_f density of saturated liquid, $\mathrm{lbm}/\mathrm{ft}^3$

ρ_g density of saturated vapor, $\mathrm{lbm}/\mathrm{ft}^3$

ρ_m density of tube wall, $\mathrm{lbm}/\mathrm{ft}^3$

$\emptyset$ ratio of heat flux to heat flux at which natural oscillation

             begins

ω carriage oscillation frequency, cycles/min

ω_N frequency of natural flow rate oscillation, cycles/min.